

Analyses of petrified wood by electron, X-ray and optical microprobes†

JAS

Journal of
Analytical
Atomic
Spectrometry

Andrzej Kuczumow,^a Bart Vekemans,^b Olivier Schalm,^b Walter Dorriné,^b
Pierre Chevallier,^c Philippe Dillmann,^c Chul-Un Ro,^d Koen Janssens^b and René Van Grieken^{*b}

^aFaculty of Chemistry, Maria Skłodowska-Curie University, 20–031 Lublin, Poland

^bMicro- and Trace Analysis Centre, Department of Chemistry, University of Antwerp (UIA),
B-2610 Antwerp, Belgium

^cLPS, CEN Saclay et LURE, Université Paris-Sud, Bat 209D, F-91405 Orsay, France

^dDepartment of Chemistry, Hallym University, Chuncheon, 200–702, Korea

Received 28th August 1998, Accepted 27th November 1998

Samples of petrified wood of different origins were analyzed by the use of the electron microprobe, capillary X-ray fluorescence microprobe, synchrotron capillary X-ray microprobe and optical microscope, applied in a microprobe manner. The main attention was given to the investigation of the ring structure of the petrified wood and the comparison of this with the ring structure of the living trees analyzed by much the same methods. The continuous X-radiation, applied in a microprobe manner, the distribution of the gray-scale representation of the secondary electron intensities and the characteristic X-ray signals, mainly from the light elements, were registered by the use of the electron microprobe method. The X-ray capillary microprobe detected the Rayleigh and Compton signals, scattered from microareas of the samples, and the characteristic X-ray signals, mainly from the heavier elements. In the synchrotron-based capillary microanalytical measurements, one of the most important results was achieved by the microprobe application of scattered synchrotron radiation. The emission and scattering results were supplemented by transmission measurements, where possible. All the methods proved to be complementary in the analysis of such periodic structures as tree rings. Both capillary microprobes were much more efficient in the detection of heavy elements and penetrated deeper than the traditional electron microprobe. Careful analysis of different signals indicated that some samples of petrified wood in the authors' possession, composed of silica of variable density, are the chemical negatives of the primordial living wood. This is the first such observation in the literature. Microdiffraction studies of the samples proved that polycrystalline α -quartz was the main matrix component of all these samples. The elemental analysis of the petrified wood gives important indications about the petrification processes. Comparison of the particular ring structure of the petrified wood with the ring structure of living trees shows great similarities. The widths of rings, density variations and density maxima are easily readable from the microanalysis of petrified wood. These parameters potentially can be exploited for the investigation of the biological, chemical, chronological and climatic information included in the fossilized tissues.

Introduction

Analyses of wood have attracted great interest for centuries, and there has been a renaissance recently, coupled with progress in modern optical and especially X-ray techniques. It has been reported that the structure of wood preserves much important information, and the ring structure of wood seems to be of special interest. The data which can be extracted from tree rings include dating^{1–5} (each ring can be identified and coupled with the annual increase in the biomass), nutrition conditions, information about pollution, detailed climatic data (overall kind of climate,⁶ temperature and precipitation^{7,8}) and previous volcanic activity.⁹ Similar data can be extracted from many natural deposits which are characterized by annual increase patterns, *e.g.*, coral skeletons,^{10–13} hard clamshells,^{14,15} stalactite and stalagmite structures,^{16–21} ice-core deposits^{22–24} and marine sediments.^{25,26} Measurements of the density and chemical composition are of great significance in the field of tree ring research. The fundamental question is how sensitive our probes are towards the changes in composition/density/topographical details and how many steps within the radial size of the ring can be made to obtain a sufficiently detailed

image of the ring. Smaller steps allow penetration of the intraring structure, giving information about the seasonal changes in, *e.g.*, temperature. Previous research with X-ray microprobes enabled the changes to be traced with an accuracy corresponding to a decade change in the living wood density.²⁷ On the other hand, scanning in small steps makes a spectrum randomized and obscure, preventing the extraction of important general information. In extreme cases, excessively detailed scans demand averaging, which obviously contradicts the earlier decrease in the step size.

Different kinds of X-ray microprobe methods have been applied in research on living wood structure. The first attempts were made by PIXE.^{28–30} Later, an X-ray capillary microprobe was used.^{27,31} The electron microprobe has not been applied in the field, probably because it demands extensive sample preparation and a vacuum is essential. While PIXE microanalysis allowed the tracing of ring structures by scanning the contents of different trace elements by linear or area mappings, the X-ray capillary microprobe introduced a new approach, the use of scattered Rayleigh or Compton radiation for density determinations. Especially, linear scans of the density were of interest. One can understand this, since the most important information is coupled with one dimension only, namely that radial to the trunk axis. It has been proved that for trees growing in Polish or southern Swedish conditions, the intra-

†Presented at the Fifteenth International Congress on X-ray Optics and Microanalysis (ICXOM), Antwerp, Belgium, August 24–27, 1998.

ring density patterns strictly followed the changes in the warm period temperature distribution. The intra-ring patterns in northern Swedish *Picea abies* wood had different structures. Their density patterns followed only the very short summer's biological activity, characteristic of the northern regions. The dark wood zone was greatly shortened in total ring structure. Thus, X-ray methods allow not only tracing of the long-term patterns of ring distribution, which has been applied in chronology and climatology for many years, but also tracing of the short-term, sub-year or seasonal changes in rings, strictly correlated with temperature variations. If it is possible to examine the wood ring structure of recent trees, it would be even more interesting to examine the ring structure as it is preserved in petrified wood.

Petrified wood is known in many regions of the world, especially the USA (Arizona, Texas), Argentina, Antarctica, Mongolia³² and the Sahara. It is recognized as an important geological witness of earlier biological activity. Some of the samples are considered to be as old as well over 200 million years, but examples of pieces only a few hundred years old are also known. Petrified trunks from the Sahara and Arizona deserts and Antarctica provide information about the biological life existing in places where nothing is now growing. Major natural collections of petrified forests are now available in some national parks (USA, Argentina). Cross-sectioned pieces of wood are prized for their beauty, especially if saturated with heavy metal oxides. Nevertheless, where the petrified wood is used for dating, pieces with clear and simple ring patterns and without disorders and inclusions are preferred.

The petrification (fossilization) process is a peculiar phenomenon from the biological and geological points of view. In general, the petrified wood is found in the silicified form; however, specimens transformed into calcite,⁶ pyrite or charcoal are known also.³³ Because the silicified form is far more prevalent and probably better preserved than others, it was adopted as an object of our research. Two mechanisms responsible for a silicification process are known. In the first, the tissue underwent decay in a moderately hot environment, rich in minerals. The organic tissue was simply replaced by inorganic, silicon-rich matter. In that kind of process only the sequence of rings is preserved, reproduced in the new material. One can call this kind of process the 'replacement process'. Dark colored samples analyzed by us seemed to belong to this kind of fossil. Another kind of petrification occurs when a solution containing some mineralizing chemicals, such as dissolved silica³⁴ and potassium and sodium silicate, penetrates the tissue, not replacing it, but impregnating it. Then not only the general pattern of rings, but also even the patterns of tissues and cells are conserved. This process can be called an 'impregnation process'. The remains of this process are clearly observable in some of our beige-colored samples. The natural process often involved a balanced contribution of these two mechanisms. In many cases the trees were covered with ash from a volcanic eruption³⁵ and conserved in that way. Later, they were covered and saturated with water (*e.g.*, in a lake or spring) and soluble Si compounds, most probably diluted silica and alkali silicates, impregnated the tissue material. The volcanic ash is a probable source of the silicon compounds. The spring waters in regions of great seismic activity (Yellowstone, New Zealand and Kamchatka) leach the silicon compounds from the lava and ash and include considerable amounts of soluble silica and silicates. Then the material is transformed from dissolved silica and alkali metal silicates into insoluble Si compounds, SiO₂ being the most common.

It has been discovered that one can imitate the natural process by the impregnation of living wood with a laboratory-made solution, composed of, *e.g.*, sodium or potassium silicate dissolved in spring or volcanic water, rich in some metallic ions and with an addition of citric or malic acid. This solution

transforms into gel but only after the penetration of liquid into the tissue.³⁶ There have also been other similar reports announcing the easy transformation of the wood into a fossilized-like form.³⁷⁻³⁹ The conditions existing in such artificial solutions were found to be similar to the conditions existing in places of great volcanic activity. Indeed, the petrification process at Yellowstone National Park occurs at a rate of 1–4 mm yr⁻¹.⁴⁰ However, the process as such obeys a very subtle equilibrium, because probably even very small changes in the environment can provoke the uncontrolled precipitation of silica; then nothing is preserved of the primary wood structure. The main disrupting factors include a sudden increase in heavy metal content, change in pH of the solution and thermal shocks. A recent report by Carroll *et al.*³⁴ describes the precipitation of amorphous silica in the temperature range 60–120 °C in both laboratory and field experiments. It has been established that there are surface defects and surface nucleation centers which control the rate of the process in supersaturated and trace element-rich solutions. During the geological scale of time, the primary hydrated gel transforms into an opal-like structure and finally into a polycrystalline quartz (chert) form.^{37,41} The transformation process takes about 40 million years in natural conditions and is the single secondary process widely described. There are many other secondary processes leading to the reshaping of the structure and composition of petrified wood, but such transformed objects are not of particular interest.

The aim of this research was to detect if any kind of information, which is observable by the naked eye on the cross-section of a petrified tree, namely clear remnants of tree rings, can be observed by instrumental methods and quantified. We selected the tools that should normally be used in research on fresh tree rings, *i.e.*, the electron microprobe and X-ray capillary microprobe. With sufficient spatial resolution, these methods should yield detailed scans of the ring and intra-ring structure. One can then compare the structure patterns with those of living wood. If they are very similar, then the conclusions drawn for modern living trees might be carefully matched with petrified wood scans. Some modifications to the techniques and methods applied in studies of fresh wood will be suggested to meet the limitations imposed on such a specific kind of material as petrified wood. To our knowledge, linear scans of such samples have been made up to now only with the use of optical microprobes and never with the use of electron or X-ray microprobes; elemental scans have never been made.

Experimental

Samples

Several samples of petrified wood were collected for our research. Two of them were from the collection of the Higher School of Farming, Agriculture Academy, Warsaw, Poland. One is beige in color, typical for a silicon oxide-rich composition (indicated below as S1). The second is dark brown, indicating a greater level of mineralization by saturation with heavy metal oxides (S2). The third piece was taken from the natural reserve in Siedliska village, very close to the Polish-Ukrainian border. This piece is also beige, with well-preserved tree rings in the outside parts, with sand-like sediments observed inside (S3). Several other samples (labeled S with further numbers) were obtained from a private collector during the Antwerp Exhibition of Minerals, Minerant, 1998. These were dug out in Hoegaerden, Belgium, and belonged to the local geological formation called Landeniaan (or more generally Maestrichtiaan) from the end of the Jurassic era, 75 million years old. The species to which they belonged are

assumed to be *Dynoxilion silvestri*. All the pieces from Belgium resembled visually the beige samples S1 and S3 from Poland.

The samples were prepared for analysis in such a way that the pieces were cut from the mineralized trunk fragments with a diamond saw. Pieces were cut in a manner to reveal surfaces perpendicular to the trunk axis and at the same time radial to the tree rings. Fragments that were sufficiently large were cut off and presented to the beam after slight polishing. The smaller cut off pieces were embedded in resin. The surfaces to be analyzed were polished with corundum abrasive papers of steadily decreasing grain size. The final polishing was effected with the use of fine diamond powder rotating targets, with the grain size of diamond powder decreasing from 15 to 1 μm . This kind of preparation was sufficient for analysis by capillary X-ray spectrometry. For electron microprobe analysis, the surface had to be covered with a thin conductive graphite layer. For microdiffraction measurements, the bulk samples were polished on one side and the next 0.7 mm thick layer was cut off, with the cut surface parallel to the polished surface.

Even after careful preparation, the samples had some defects. Especially, the ring boundaries were filled with a brittle material, which was in many places removed, with openings left. This demanded careful selection of the scan location, great care during the analyses and special attention during the data treatment. Unfortunately, the relatively small pieces of our material did not allow the analysis of very long sequences of petrified tree rings (over 40 rings).

Instrumentation

The samples were analyzed by the use of different micro-analytical devices. The first was IMIX (Integrated Micro-analyzer for Imaging and X-Ray), produced by Princeton Gamma-Tech. It was a scanning electron microscope with an energy-dispersive Si(Li) detector. The working voltage for the electron gun was always set on 20 kV. The line profile analysis option was selected to make linear scans through the samples. This option was mostly dedicated to match a material such as tree rings, in which the most important information is included in the radial profile. The searched field of view was selected using the image obtained from the secondary electron signals. The image extracted from the secondary electron signals was preferred, because the topographical orientation on the sample was essential for coupling the chemical information with surface details. The line scan was performed across the center of the image. The orientation of the image was selected in such a way that the scan proceeded perpendicular to the trunk and radial to the ring direction. The radial direction was followed outwards. The secondary electron image of the sample was stored to establish and control the location of other measurements to be continued on the same sample. This image was also used in our analysis in another way. A gray-scale level distribution along the line of scan was made. The gray-scale morphology diagram in its raw form was difficult to analyze but, after smoothing of data points, the internal structure of the scanned area was revealed. All the samples analyzed by the scanning electron microprobe were thick. We could not prepare samples thinner than several hundred micrometers and the penetration depth of this kind of microprobe was not greater than 5 μm .

A tabletop X-ray capillary microprobe was the second option for the analysis. The device was built in the Department of Chemistry at the University of Antwerp (UIA), Belgium, and has been described in detail elsewhere.^{42,43} A Siemens rotating anode Mo tube was used for excitation. The X-ray beam was squeezed to the size of the outlet capillary diameter, *i.e.*, 15 μm . Since the distance from the outlet to the sample was relatively large (about 1.5 mm), the effective beam size was at least double the above value. The sample was driven

in front of the capillary outlet by a set of four computer-controlled step motors. A linear scan was again the preferred option; thus only one motor was effectively working, except at the moment of initial positioning of the sample. An Si(Li) detector was applied for the detection of the fluorescent and scattered radiation and an NaI(Tl) scintillation detector for the registration of the transmitted radiation. The scans were made on samples that were as thin as allowed by the sample preparation technique (about 1 mm), in order to avoid an excess of scattered radiation, the intensity of which is proportional to the thickness of the sample and more than sufficient for the analytical aims. The brittleness of the material prevented further thinning of the samples. However, the thickness of the samples was uniform and under control to within 10 μm .

The synchrotron measurements were performed at the 4.45 GeV positron synchrotron in HASYLAB, Hamburg. Beamline L was used, but the primary beam was attenuated by the introduction of an 8 mm thick Al sheet. Other restrictions were imposed on the final beam size by installing a 10 cm long straight capillary of 30 μm id. The energy range of the primary beam was between 1 and 100 keV. The secondary radiation was registered with an HPGe detector. The fluorescent lines and also the selected channel in the scattered white synchrotron radiation (38.5–53.5 keV) were chosen for the collection of the data.

All the scans, regardless of the method applied, were carried out on the same samples and at locations as close as possible in order to obtain comparable results. However, the different methods of sample preparation and different times and places of analysis did not allow strictly the same positioning for different methods. The lengths of the scans were comparable, but they could sometimes differ in the position perpendicular to the length direction by as much as several hundred micrometers. Because the ring structure is not strictly parallel, this sometimes gives a slight shift in the ring width.

In general, the electron microprobe can deliver a better spatial resolution than the X-ray capillary microprobe (even up to three orders of magnitude). The depth penetration and the information volumes are totally different (the depth penetration of the material for the electron microprobe is of the order of a few micrometers whereas for the tabletop X-ray capillary microprobe it reaches 1 cm and for the synchrotron version it even exceeds 5 cm). The electron microprobe brings information more concentrated on the low-Z elements, whereas the two X-ray capillary microprobe versions are much more sensitive for heavy element determinations. Hence, the electron microprobe brings results that are strictly surface-orientated, whereas the X-ray microprobes give a much deeper insight into the sample. Still, if the results can easily be compared with the same structure observable in all kinds of scans, this testifies to the uniform general features of the petrified ring structure. Brief details of the methods applied are given in Table 1.

The microdiffraction measurements were made on an X-ray microprobe at LURE (Orsay, Paris). It was installed on the D15 beamline at the DCI storage ring. This installation has been described elsewhere.^{44,45} The 10 keV photons were extracted from the white synchrotron radiation and, after passing the input diaphragm, focused with the Bragg–Fresnel multilayer lens to a focal spot 20 μm wide. The diffracted radiation was registered in the transmission mode on a 2D-CCD 'imaging plate' made by Fuji. The image from the plate was scanned with a Molecular Dynamical scanner and stored as an image-type data file. After the image integration, the diffraction 2θ pattern was extracted. It can be matched with the library of the diffraction patterns or processed for phase identification.

Table 1 Details of the methods applied

Microprobe method	Spatial resolution/ μm	Steps applied/ μm	Penetration depth/ μm	Detectable elements	Auxiliary signals
Electron	< 1	50	< 5	Na–Ca	Bremsstrahlung
Tabletop X-ray (capillary)	15–30	100	Up to 10 000	Ti–Pb	Rayleigh-Compton
Synchrotron X-ray	> 30	50	Up to 50 000	Ti–Pb	White

Results

The measurements by the electron microprobe gave different results. The linear scans made on sample S2 gave very clear indications of preservation of the primordial ring but not cell structure. The scans made on samples S1 and S3 were much more obscure; however, careful analysis helped to reveal the essential details also. In general, the faint brown samples S1 and S3 turned out to be much less ring ordered and mineralized than the dark brown sample S2. Otherwise, the primordial tissue structure was preserved only in beige-colored samples.

The electron microprobe analyses revealed the main composition of the samples, which was surprisingly uniform even on a macroscopic scale. Silicon dioxide was the most prevalent component, with other elements clearly noticeable, but at low levels: Cl, S, P, K and Ca. The K lines of these six elements were selected after the initial selection as the separate measurement channels; one additional channel was added in the position of the intensive bremsstrahlung in the range 2.9–3.0 keV. The latter channel was selected to make the information more oriented to the density variations, thus comparable to those obtained from scattered signals in XRF. Statistically significant lines of heavy metals were absent in the electron microprobe measurements. This was striking, because each sample was clearly colored, especially the dark brown sample S2. Of course, the high bremsstrahlung background restricts the possibility of the detection of an element if it is present in concentrations below a few hundred ppm. The X-ray spectra taken for all the samples were very similar, indicating that the macroscopic composition of the samples was very simple and uniform. Much greater differences were observed in the optical branch of the spectrum, even with the naked eye.

The results of the electron microprobe measurements on sample S2 are shown in Fig. 1. The Si line and bremsstrahlung channel contents follow the ring structure of the wood, showing the dark and light parts of the rings. The K line intensity follows the same pattern [Fig. 1(a)]. The level of the correlation between the three lines showed that they could be used in an exchangeable way to reveal the essential ring structure of the tree. For example, the parameter τ in Kendall statistics has the value 0.596, while the probability parameter is very close to zero, indicating a significant correlation. The Ca line intensities follow a much more complicated pattern [Fig. 1(b)]. The average (threshold) contents of this element are correlated well with the above-mentioned lines of the K, Si and bremsstrahlung channels. On the other hand, in many scan positions, the levels of calcium are clearly elevated, which may indicate some small inclusions. In this respect the behavior of this element is very similar to that in living trees.³¹ Even the geometrical diameter of the inclusions (50–120 μm) is similar to those described in real wood. It is even probable that some part of the Ca content, just related to the elevated levels, had its origin in the Ca content of the primary wood material and was not exchanged during the petrification process, but just conserved. This opinion can be justified additionally by the fact that inclusions are buried deeply inside relatively uniform silica zones. This contradicts the supposition that the inclusions might be the results of secondary processes. Such potential secondary processes would transform the whole of the rest of

the structure, which is not a fact. The average Ca concentration is highly correlated with those of S and Cl and, to a smaller extent, with that of P [Fig. 1(c)]. This level of correlation might show that small amounts of Ca in the petrifying solution were present as a mixture of calcium sulfate and chloride. However, in locations with locally elevated Ca contents, the correlation with Cl no longer holds. Some of these elevated levels of Ca are clearly associated with the presence of S and others with P. Small inclusions are then inclusions of calcium sulfate or phosphate, never together. In contrast, the K contents are relatively well correlated with the chloride and phosphate concentrations.

It was impossible to establish, on the basis of electron microprobe measurements, the real physico-chemical reason for the differences between the dark and bright locations on the wood cross-section. They certainly followed the tree ring pattern of living trees, but the chemical composition was totally determined in this case by the presence of SiO_2 . The great differences, especially in the bremsstrahlung and Si signals, could be related to the variability in the density of the material. In the same way it was difficult to decide what kind of trace heavy metal cations caused intensive coloring of the samples. Maybe microscopic metallic clusters were the source of the coloration. Alternatively, it was even possible that no single heavy element was responsible for coloring the samples and the reason lay rather in the degree of silica hydrolysis or in structural defects.

The scan direction had earlier been established by the use of the secondary electron image. The secondary electron image was preserved and transformed into the gray-scale image. The gray-scale distribution was established along the scan line. The raw gray-scale morphology data were noisy and only after filtering did they reveal the internal structure. This was strictly the ring structure of the petrified wood as shown in Fig. 2. The degree of qualitative similarity in the total pattern is striking; however, there are also serious differences in the intensity of the Si and bremsstrahlung on the one hand and the secondary electron signals taken from the electron microprobe measurements on the other (see the right side of Fig. 2). Maybe the discrepancy in the intensity of these kinds of signals is a measure of the surface quality. We should remember that the secondary electrons are extremely sensitive to topographic details.

The analysis of the typical beige-colored sample S3 by the use of the electron microprobe did not give such conclusive results (Fig. 3). The count rates for the determination of the different spectral lines differ from those in the previously described case. However, the lines of the main matrix components (Si, K and the bremsstrahlung channel, expressing the matrix features of the samples) were much the same as for sample S2. This shows that the differences in matrices were not great, with silica once again the main component. More differences were seen at the level of the minor elements: the Cl and P signals were on average two times weaker in this case, the Ca signal two and a half times and the S signal four times in comparison with the values registered for the S2 sample. The ring structure was not as pronounced as in sample S2, even by tracing the lines of the main components. The signal of Si was much clearer than the others, with the ring

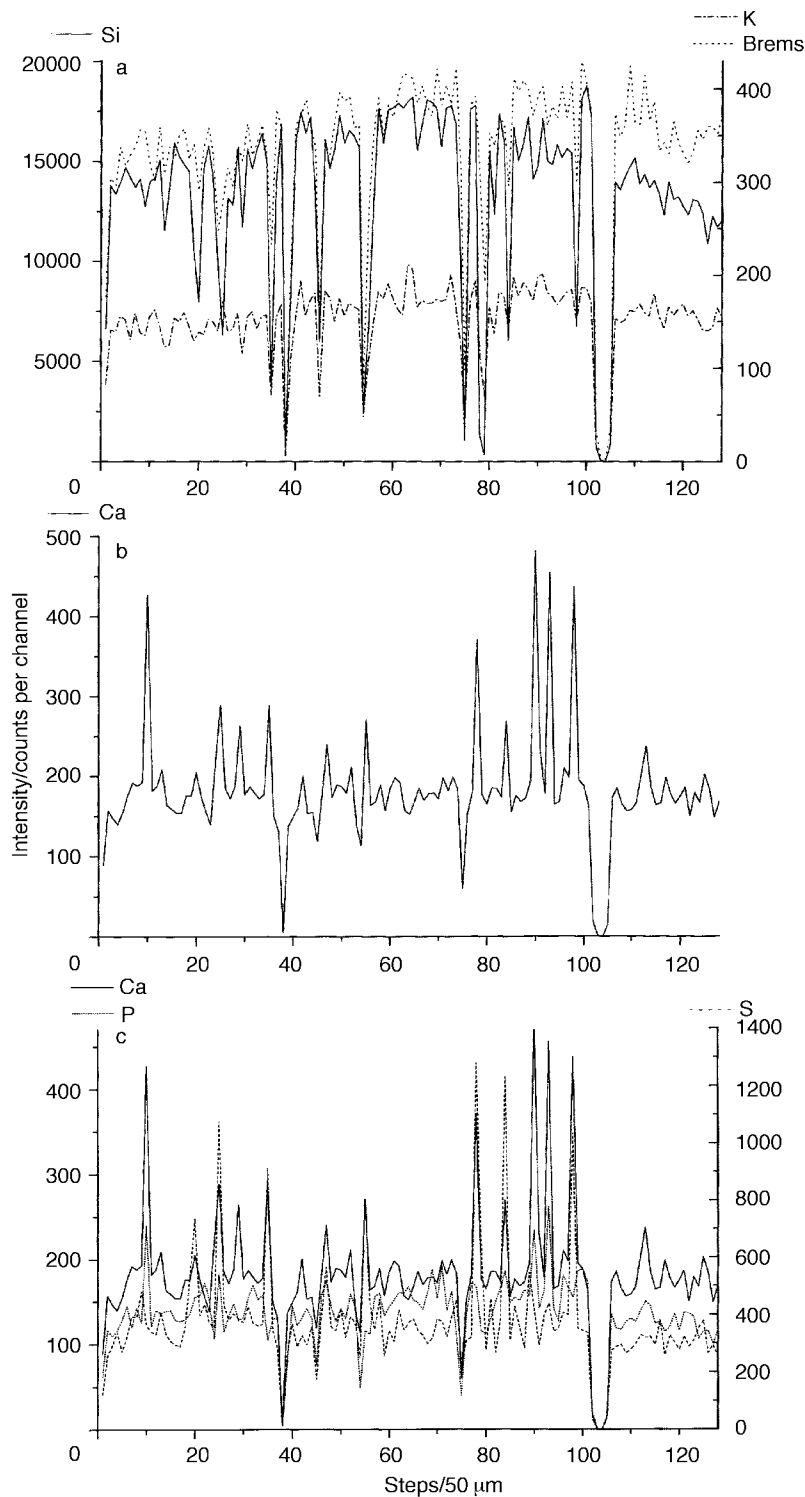


Fig. 1 Electron microprobe scans of the petrified wood sample S2. (a) Correlation between the signals of Si, K and the selected channel of the bremsstrahlung radiation (2.9–3.0 keV); (b) calcium levels, with the inclusions clearly noticeable; (c) association of the elevated Ca levels with the sulfate or phosphate contents.

structure very clear, but the intensity of the signal dropped by more than 20% on going to the region with much more pronounced inclusions.

The bremsstrahlung signal was somewhat obscure when considered on its own. It was helpful to analyze the diagram of the continuous radiation in parallel to the Si curve [Fig. 3(a)]. The bremsstrahlung signal was not as sensitive as the Si signal to the changes in the granulation of the sample. This shows that the density of the matrix in the inhomogeneous regions was much the same as in the rest of the material. The

real drops in the density were in the regions of the dark wood, reaching 30% of the maximum value. This was similar to the values observed for those rings in sample S2. It is worth noting that in sample S3 the internal splits and brittleness of the material did not affect the drops in the Si signal. The distribution of the K signal was not as correlated with the bremsstrahlung and Si signals as in sample S2. Similarly, the Ca signal was rather uncorrelated from the main component signals [Fig. 3(b)]. Still, sudden increases in the Ca level occurred more frequently in this part of the sample where the

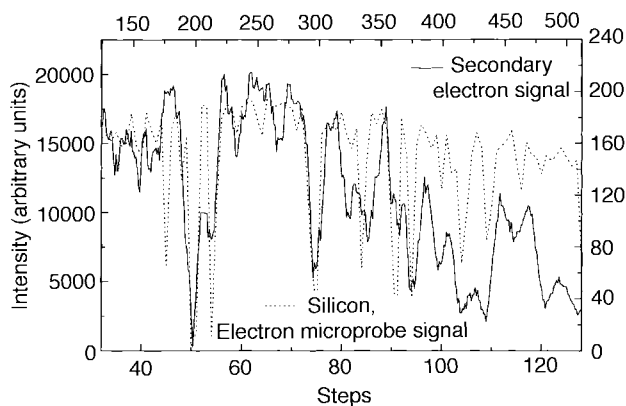


Fig. 2 Gray-scale distribution of the secondary electron intensity levels (solid line) along the line of the scan from Fig. 1 (in steps equal to 12.5 μm)—right scale. The silicon signal is shown for comparison (dotted line) (steps 50 μm)—left scale. Electron microprobe analysis of sample S2.

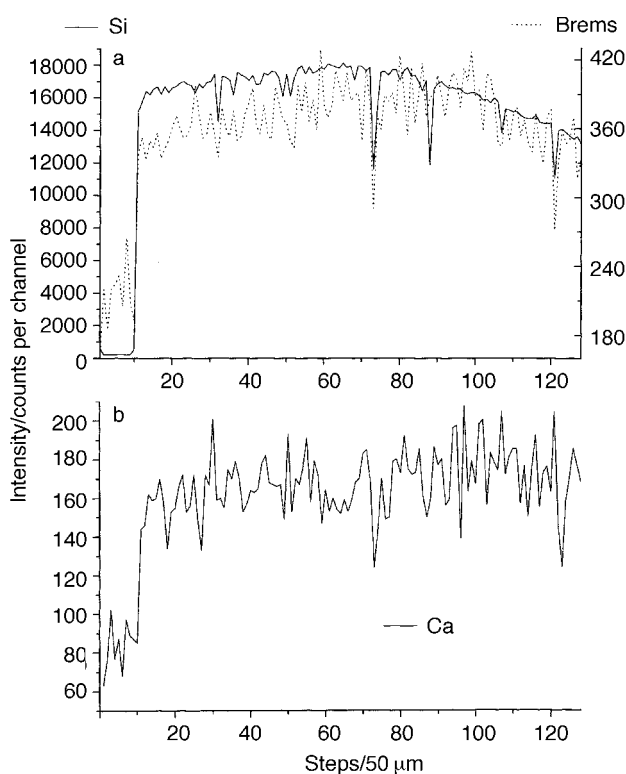


Fig. 3 Electron microprobe scan of sample S3. (a) Correlation between Si and selected bremsstrahlung channel signals; (b) calcium signal.

granular structure was pronounced. The correlation between the Ca, S and Cl levels nearly disappeared. A slightly better correlation could be observed between Ca and P. Much better but still far from ideal was the correlation between K and all three anions.

The measurement of sample S2 by the tabletop X-ray capillary microprobe gave another series of results (Fig. 4). The most important among them were the spectra of the coherently and incoherently scattered tube Mo $K\alpha$ line and the lines of some metallic components of the petrified wood. Rayleigh, Compton [Fig. 4(a)] and Si signals followed the ring patterns and could be treated in an exchangeable way. Still there are some differences between the signals: the Compton signal seems to be less sensitive to the local changes in the density of the petrified wood, giving an averaged picture of the rings. The Rayleigh scattered and Si characteristic signals

are much more bound to the local changes in density, giving some additional substructures on top of the main ring structure. The additional substructures had a different degree of correlation—sometimes the Rayleigh signal followed the changes in Si signal and, in those places, the variability of the matrix seemed to result from the changes in silica, whereas in other places the subsignals were not correlated. The differences in the Rayleigh and Compton spectra can be fully understood taking into account the features of these kinds of scattered radiation.^{46–49} On average, the ratio of the Rayleigh to the Compton signals was constant through the scan, testifying to the constant mean atomic number of the matrix, determined totally by the silica. The discrepancies are very small.

Similar to the analysis by the electron microprobe, the levels of Cl and S were interrelated and they were also correlated with the levels of Ca (not shown here). Especially striking was this correlation in the places where the levels of Ca were elevated in a very significant way.

The X-ray capillary microprobe allowed the tracing of the signals of some heavy elements present in the samples of petrified wood (Ti, Fe, Cu and Zn in amounts reaching several tens of ppm and Mn, Ni and Pb at concentrations in the ppm range). All of them concentrate very clearly at the sites of the dark wood (minima in Rayleigh, Compton and Si signals). It gave the total metallic concentration at a level of many hundreds of ppm. The increase in the heavy metal contents [Fig. 4(c)] is not followed by an increase in the contents of anion-creating substances [Cl, P and S; Fig. 1(c)]. It obviously would demand much greater amounts of anionic elements than those detected. Hence it can be concluded that heavy metals in the parts of petrified wood imitating the dark wood are mainly in the oxide form or as silicates. Fe, Ni and Zn also have some smaller, irregular and grain-like inclusions in the places corresponding to the light wood in living wood, similar to the behavior of Ca. This is analogous to the results of the analysis of living wood.^{31,50}

Additional measurements were possible by the application of the transmission technique in X-ray capillary microprobe mode. The result is shown in Fig. 4(b). The reversed transmission scan shows a striking similarity to the direct Rayleigh or Compton spectrum.²⁷ The transmitted radiation is inversely proportional to the density of the material; if the reversal of the transmitted signal is equivalent to the scattered signal, then the latter should be directly proportional to the density. The higher intensities of scattered signals and the lower intensities of transmitted signals are coupled in sample S2 with the locations of earlier light (less dense) real wood. This result is important and strongly confirms our hypothesis that some kinds of petrified wood are the chemical negatives of the natural wood.

The synchrotron-based X-ray capillary microprobe was also applied. Owing to the very long optical path, this device was poor in detecting low- Z elements, even Si. The investigation of heavier elements was much more efficient, with Zn, Cu, Pb and Ni concentrating at the locations of the primordial dark wood ring boundary [Fig. 5(b)]. In addition, the application of the wide channel selected from the background synchrotron radiation (38.5–53.5 keV) brought interesting results [Fig. 5(a)]. The scan based on this radiation enabled us once again to trace the density structure of the petrified wood, giving full analogy with, *e.g.*, the Rayleigh or Compton scans from the tabletop X-ray capillary microprobe. Because of the strong contribution of the Compton (even multifold) scattered radiation to the white synchrotron scattered emission, the scan resembles more the Compton than the Rayleigh scan from the tabletop instrument [Fig. 4(a)]. The spectral resolution of both probes was similar (about 30 μm), as were the penetration

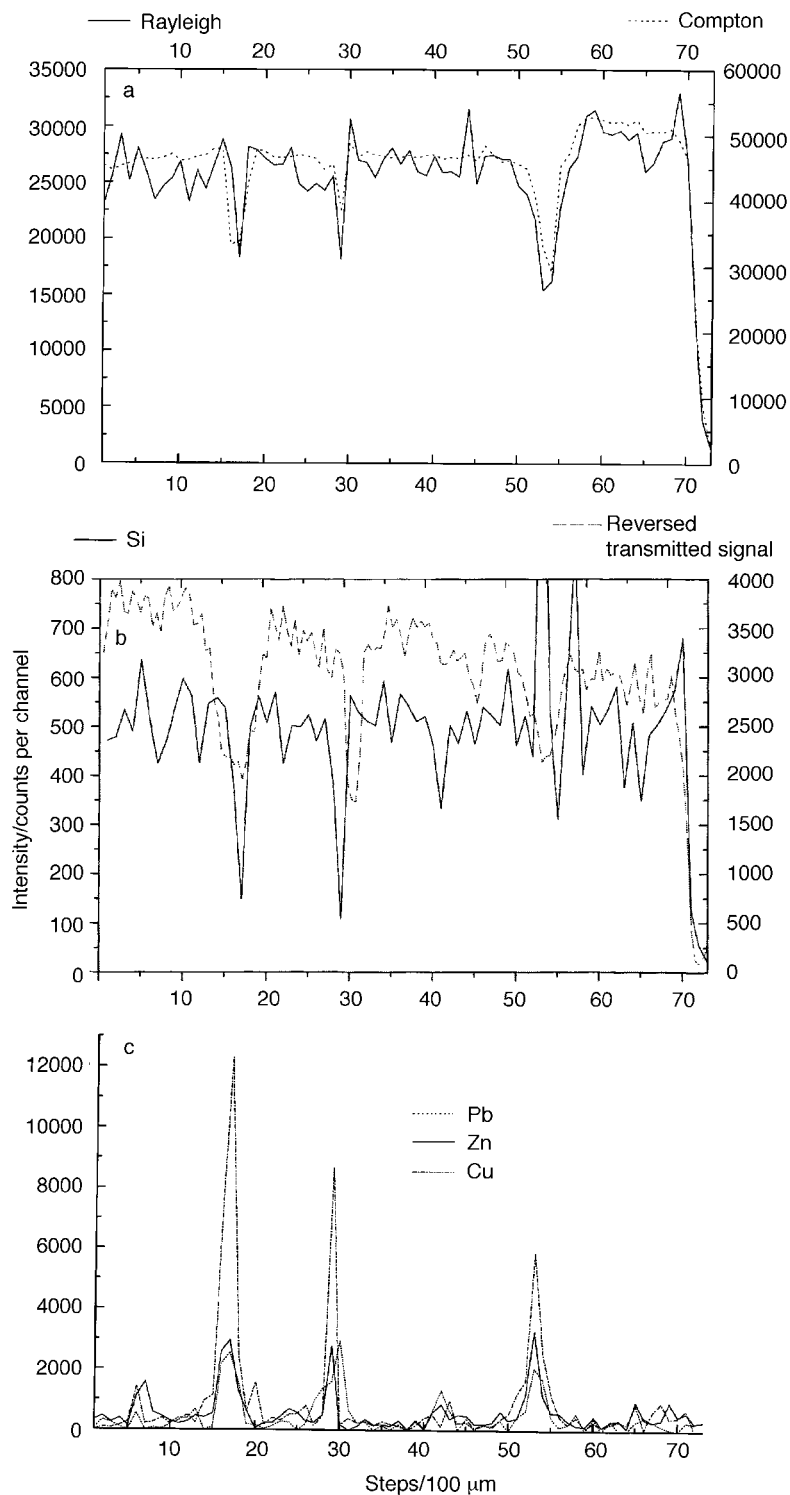


Fig. 4 Scans of sample S2 by a tabletop X-ray capillary microprobe. (a) Rayleigh (solid) and Compton (dotted) scans; (b) Si (solid) and reversed transmitted (dotted) signals; (c) heavy metal scans (Pb, Zn, Cu).

depths (order of centimeters), and did not add any differences to the scans.

Comparisons between microprobes

We compared the Si signals, the bremsstrahlung channel from the electron microprobe, the Rayleigh signal from the tabletop and the scattered white signal from the X-ray synchrotron microprobe, measured for the same piece of petrified wood S2. We should remember that the samples were prepared in different ways (thick sample for EPMA and thin sample for μ XRF) and that the scans were carried out at close but not

identical locations. Careful analysis of Fig. 6 shows the similarities in the Si scans for the samples and the less pronounced similarity between the bremsstrahlung and Rayleigh spectra. They can certainly be treated as exchangeable if the conditions of the sample preparation and analysis were set strictly the same. Still, we can see some specific differences, resulting from the nature of the sample and the specific features of the analytical methods used in this study. One can see in the Rayleigh spectrum (and also in the Compton spectrum in Fig. 4) only one wide ring (second from the right). The bremsstrahlung and secondary electron spectra show two ring structures at the same location. Silicon spectra, taken both

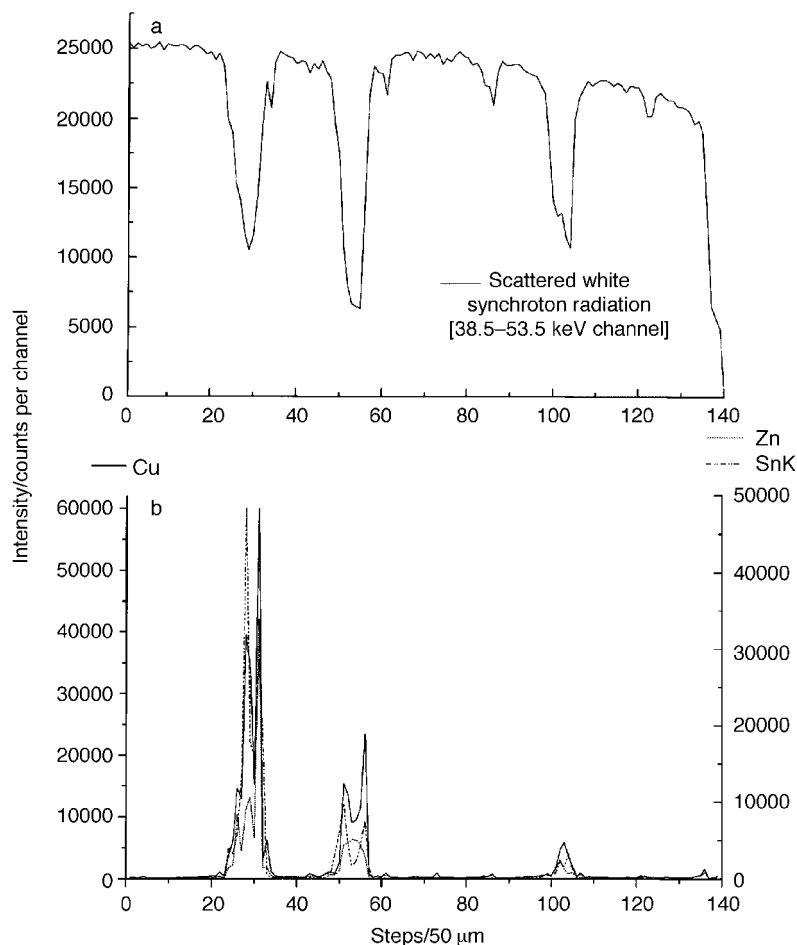


Fig. 5 Synchrotron-based X-ray capillary microprobe scan of sample S2. (a) Application of the selected channel (38.5–53.5 keV) for the scan; (b) heavy element presence in the petrified wood structure.

from the electron and from the X-ray microprobes, show two rings, much better presented on the electron microprobe scan. This discrepancy can only be explained when we assume that for some reason the ring structure in this location is fully represented only in the shallow surface region, of the order of the depth of the electron penetration (hence of the order of 5 μm for 20 keV electrons, used in this work). The probes, which are penetrating very thin layers, can easily detect it. The deeply penetrating X-ray microprobe averages the signals on going from the deep to shallow layers. For photons with an energy of the order of 20 keV, *e.g.* the Rayleigh and Compton photons originating from the Mo $K\alpha$ radiation, the contribution of the micrometer deep layer is not noticeable in the total balance of the detected photons. Their penetration depth in SiO_2 is of the order of 8500 μm . One cannot differentiate the uppermost layers by those signals. The same holds for the selected channel in the synchrotron background radiation, of energy between 38.5 and 53.5 keV, the radiation from which can penetrate the sample by over 50 000 μm . However, by using the Si characteristic radiation, the mentioned additional ring structure can be detected in the X-ray capillary microprobe. In this case, the signal is collected from a depth determined by the Si $K\alpha$ (1.7 keV) escape length, thus from a depth of about 30 μm . This signal is still better seen in the electron microprobe measurement, where it is collected from the depth governed by the electron range. That distance (about 5 μm) is probably still better suited to the real depth of the structure than the Si $K\alpha$ escape length.

The next detail, which can be seen by comparison of spectra from different devices, is the different sensitivity of signals to the local changes in the samples. On average, the secondary

electron and all other electron microprobe signals are much more 'noisy' than the spectra from the X-ray capillary microprobe. This can be explained from various points of view:

(i) the X-ray capillary microprobe certainly has a worse spatial resolution than the electron microprobe; hence its work resembles the averaged electron microprobe scan;

(ii) the electron and secondary electron microprobes are much more sensitive to all the minor roughnesses on the surface of the sample, resulting both from the sample preparation and from its brittleness;

(iii) owing to its deep penetration, the X-ray capillary microprobe averages the influences on the signal both from the shallow and deep roughness.

For example, in the electron microprobe-based fluorescent and secondary electron spectra of one ring structure, one can see a number of oscillations and jumps, which are hardly or not observable in the X-ray capillary spectrum. We can attribute them to the uneven locations on the surface or to the slightly spongy structure of the material. Everything is averaged by the robust manner of the data collection in X-ray capillary microprobes, both the tabletop and synchrotron-based types.

Microdiffraction measurements

The microdiffraction measurements of the bright and dark locations on samples S2 and S3 were made using the LURE facility. As the different previous microprobe measurements suggested, the silica in some forms should be by far the main component of the samples. However, this matrix should vary

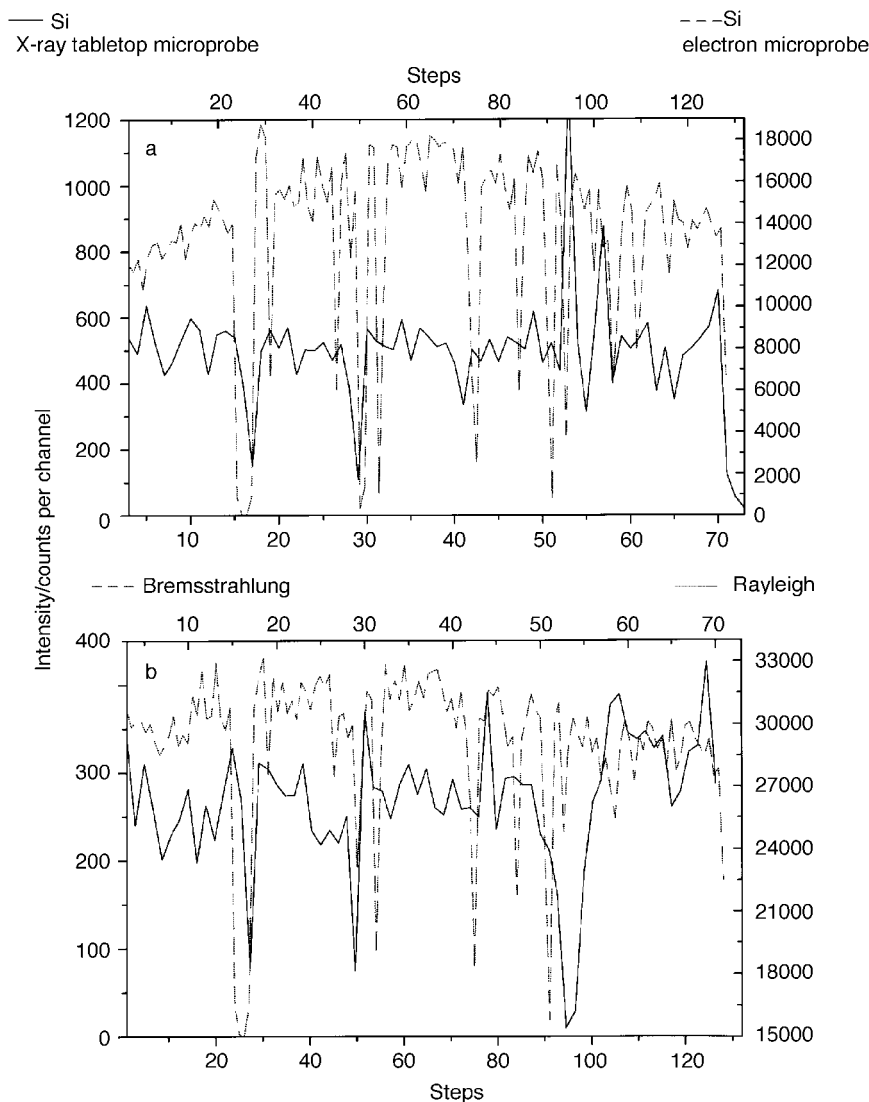


Fig. 6 Similarities in: (a) Si scans as made by the electron and tabletop X-ray capillary microprobe; (b) bremsstrahlung scan (EPMA) and Rayleigh scan (tabletop capillary μ XRF). Measurements by the electron microprobe made in 50 μ m steps, by the X-ray capillary microprobe in 100 μ m steps. Sample S2.

substantially in density in dark and bright locations. The microdiffraction measurements gave roughly the same image of the main crystallographic component for dark and bright locations in both the samples [Fig. 7(b)]. This pattern was identified by comparison with the ASTM Powder Diffraction Files as an α -quartz phase. The difference both between dark and beige wood and between dark and bright locations on each sample was in the intensity ratios of the lines of different diffraction order in the spectra. We interpreted this as resulting from the different ratios of the quartz phase to the unidentified, but probably amorphous, silica. It obviously leads to changes in the density of samples. The amount of the crystalline quartz phase should be much greater in the black sample S2. The amorphous silica (opal) will be present at increased levels in the original bright locations. The diffraction patterns were obviously ring-like [Fig. 7(a)], suggesting the existence of the polycrystalline phase each time. Our concept of the structure of the petrified wood is as follows:

- (i) fine-grained α -quartz is the main component;
- (ii) some amounts of amorphous opal are present in locations on the primary light wood, increasing the density of the material;
- (iii) amounts of opal are small in locations of primordial

dark structure, while the coarse-grained silica is present, which leads to loosening of the structure.

The microdiffraction measurements are in full accordance with previous independent reports.^{37,41} They seem to suggest that in the first phase of the petrification, the amorphous, opal-like structure is created, then subjected to the continuous recrystallization process, leading to the formation of microcrystalline quartz. It can, but does not need to, lead to the loss of the primary tissue structure, if earlier it has been fixed. However, it is not clear at what stage of the process the tissue pattern of sample S2 was lost. Maybe the greater amount of mineral components, both of metallic (Ca, Ti, Fe, Cu, Zn and others) and anionic (S, Cl and P) character, changed (accelerated?) the conditions of petrification and recrystallization, not allowing preservation of the original structure since the very beginning. Alternatively, the tissue pattern has been damaged during passage from the opal-like to the micro α -quartz structure.⁴¹

Conclusions

The results of the investigation fully confirmed the hypotheses about the delicate replacement of the organic tissue in wood by

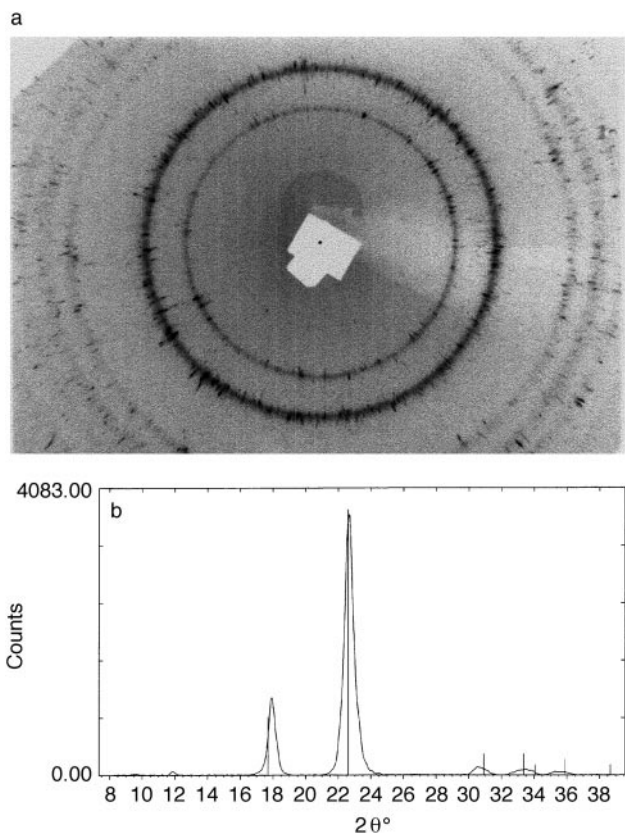


Fig. 7 (a) Microdiffraction pattern as scanned from the imaging plate. The measurement was made for the dark wood location on the black wood sample S2; the exciting beam from the D15 beamline was of 10 keV energy and 20 μm in size; (b) 2θ scan extracted by integration of the previous image.

the petrifying solution of silica and silicates, most probably a K-rich one, with a small admixture of calcium chloride and sulfate. The presence of Na in the primary solution, probable from the chemical point of view, was not confirmed by the results of our analyses. Clear indications of the second petrification mechanism, namely by impregnation, have been found, because the remnants of the tissue/cellular structure have been preserved in samples S1 and S3, easily detectable with the optical microscope. A similar situation has been found in some Belgian samples. The essential structure of all the samples is very similar, with SiO_2 in an α -quartz form by far the main constituent. On the boundary of rings, a large decrease in the Si signal occurs (up to 30%). Since the additional material filling these places is present in distinguishable but small amounts (heavy metals up to the level of hundreds of ppm, e.g., Fe, Cu, Zn), it looks as if the density of SiO_2 became lower in the location of the dark wood for the black-colored fossils (originally in the fresh wood with a greater density of cellulose). This results from the analysis of the Si, bremsstrahlung, transmission and scattered Rayleigh and Compton signals (a more detailed logical signal analysis is given elsewhere⁵¹). The said petrifying liquid, composed of an aqueous solution of silica and potassium silicate, with a threshold amount of calcium chloride and sulfate, was very sensitive to the presence of any heavier cations (including Ca) and to the internal structure of the cellulose and lignin. The cellulose in now dark-colored wood samples was substituted with the denser Si-bearing material where it was less dense and *vice versa*. The Na contents, if present at all, were probably leached from the material at the time of hardening, while some amounts of potassium silicate were preserved. Probably now it is a solid solution of potassium silicate in solidified SiO_2 , composed of fine-grained α -quartz admixed with amorphous opal. In addition, the threshold amounts of calcium chloride

and sulfate are still uniformly included in this solid liquid, easily differentiated from the Ca inclusions, the latter certainly of primordial wood origin. However, we cannot suggest that the whole Ca threshold content is of external origin; probably part of it can be accounted for by intrinsic Ca presence in the wood tissue.³¹ Maybe the diffusion plays some, but limited, role here. The boundaries of the grain-like Ca- and Fe-bearing structures are surprisingly sharp. In general, the structure of the black petrified wood can be treated as a kind of 'chemical negative' of the primordial wood structure. Similar analysis of the results concerning the beige-colored samples is not so decisive, because the auxiliary signals from the electron and X-ray capillary microprobes do not supply us with such unanimous indications. Analysis with a petrological microscope did not give any indications of the secondary geological transformations of the petrified wood. Especially, there was no proof of the calcite inclusion in the petrified wood structure. Calcium, if present at elevated levels, was always in gypsum or phosphate form.

The contents of all the other elements are small in comparison with SiO_2 . The amounts of other elements (K, S, P, Cl) are different in both kinds of samples—in the dark-colored sample S2 2–4 times greater than in the pale brown samples S1 and S3 and in the Belgian samples. It seems that a more pronounced increase in the contents of these elements would disturb the subtle equilibrium in the liquid saturating the primordial wood. Tracing the amounts of Ca seems to be especially instructive in this context. For example, increased amounts of Ca can be observed in those locations in samples S1 and S4 where the granular structure is more pronounced. The granular structure is placed inside the trunk and is surrounded by the well-preserved ring structure. It is not clear whether the trunk was petrified only in part from the outward side, the interior being intact and with organic matter inside obeying the normal decay process. Then the whole structure transformed in something like an SiO_2 pipe, with the empty interior filled with additional, granular and sand-like mass (see samples S1 and S4). These remnants within the internal structure of the log could be created in the non-volcano-related process of the petrification. Alternatively, maybe, the whole structure was transformed into the petrified form with the ring structure fully formed, but later the process of rapid secondary solidification around the Ca inclusions started. It finally damaged the ring structure inside the trunk.

On average, the degree of additional, non-silica mineral contents in the dark sample S2 is much more pronounced than in the other samples. In addition, in that sample all the components can be clearly coupled with each other: locations with the inclusions of calcium sulfate are clearly observed and can be distinguished from the inclusions composed of calcium phosphate. The threshold amounts of Ca and K are strictly coupled in sample S2 to the signals of Si, the bremsstrahlung and the scattered signals. This testifies to the uniform dissolution of the whole K and threshold Ca contents in silica. This regularity is not so clear for samples S1 and S3.

On the other hand, sample S2 seems to be mechanically sensitive in the locations of the singular ring boundaries. The low-density material characteristic of such locations is brittle and can easily be damaged, especially during the sample cutting and preparation processes. These locations are relatively saturated with heavy metal contents. Thus, the losses in material contents, fractures and even splits additionally sharpen the ring boundaries. This must be taken into account and demands special care during the spectral analysis.

The spectra in the systems bremsstrahlung, Si, K, Cl (for sample S2) and the Si or bremsstrahlung signal intensity (for S1 and S3) *versus* the scan length (or scan step number) are very similar to the scans of the tree rings in living trees. The relevant linear scans were made with the tabletop X-ray capillary microprobe.^{27,31} The tree ring shapes revealed in the

scans on living wood seemed to belong to two categories: the sharply shaped characteristic of the trees growing in the very severe conditions of northern Sweden, and mildly shaped characteristic of the wood from trees from southern regions of Sweden or from Poland. We extracted the typical shape of the singular petrified ring (Fig. 8). In Fig. 8(a), the shape of the ring of the petrified wood, as obtained from the bremsstrahlung signal, is compared with the shape as revealed from the Si signal. The similarities are striking (the Kendall τ parameter is equal to 0.269, the probability parameter for that test is 0.0878, both testifying to a significant correlation). This proves that both signals can be used in a fully exchangeable way. In Fig. 8(b) and (c), the shape of the petrified wood ring is compared with the typical tree ring shape of the moderate climate wood (b) and northern wood (c). The similarity

between the petrified and the last diagram is very pronounced. This conclusion demands checking on a more representative population of samples than that which was available for this study. Especially, the possibility that such sharpening of the figure is not an artifact resulting intrinsically from the petrification process must be excluded. Still another possibility is that, in the dark wood analogs of the petrified tissue, the brittleness of the materials gives some mechanical fracture, which itself adds to the normal density diversification, thus sharpening the boundary. However, in our opinion, the degree of the correlation between the patterns of petrified and living trees is so meaningful that we can consider the information preserved in petrified tree rings as speaking a lot about past conditions.

Finding the northern type of petrified wood in Poland is not unrealistic, for several reasons. For example, the climatic conditions changed periodically on the geological scale of time from the tropical to the polar. In addition, the Scandinavian glaciers, expanding from time to time, brought and left great amounts of mineralogical materials from the northern regions. The study by Francis⁶ of Antarctic petrified wood confirmed that there were essential climatic changes over tens or hundreds of millions of years.

Future prospects

As we have shown, the investigation of petrified wood should be an important supplement to recent research aimed at extracting the information included in various periodic structures: tree rings, ice annual layers, sea sediments, corals, stalactites, rings on clamshells. The analysis of tree rings seems to be particularly attractive in some respects:

(i) it gives us an insight into the petrification process, and in that sense it should reveal some important details of the old and recent geological processes, especially in the regions of great geothermal activity; in particular, it can be important for the search for 'cold' geological processes, where the temperatures are relatively low (below and around 100 °C) and the process goes through an array of subtle equilibrium conditions;³⁴

(ii) it shows a general pattern of tree rings, allowing attribution of the investigated pattern to the conditions of the tree growth on a 1-year long scale (microscale climatic research);

(iii) in the case where a much longer sequence of the rings is available, the ring spectra can supply us with information on the climatic variations on a scale of a few hundred years; this kind of information is now intensively sought,^{52,53} increasing our knowledge of the climate; it would be interesting to know if the medium time-scale of changes has some repeatable patterns on the geological time-scale, going from our recent knowledge of the climate to the past;

(iv) for tree rings with remnants of the tissue structure, detailed botanical studies would be possible, possibly leading to the identification of the species and to comparable investigations with the living species; the petrified structure can be easily revealed by optical and X-ray investigations, the latter allowing the addition of the elemental knowledge of the sample; some of the elemental details can be attributed to the primordial structure of the wood;

(v) finally, some kind of dendrochronological application is also possible by the use of petrified wood, as has been shown by Kumagai and Fukao³⁵ for the estimation of the volcanic activity in some areas in Japan; of course, any kind of absolute dendrochronological estimation, possible for recent trees,^{3-5,54,55} is excluded in the case of petrified material.

Climatological research involving the information included in petrified wood seems to be very valuable and one of not so many possibilities of tracing the micro- and medium time-scale variability of climate in geological epochs older than

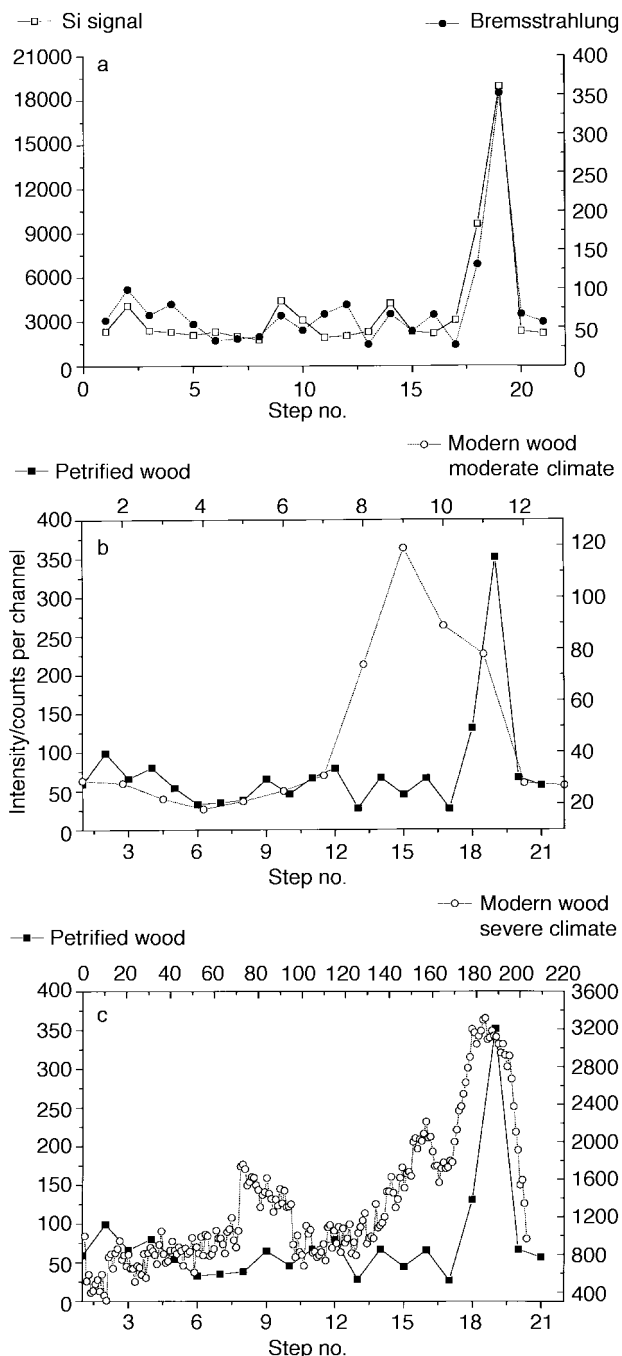


Fig. 8 Outline of: (a) the typical petrified tree ring shape (sample S2) as given by the bremsstrahlung or Si signals; (b) fresh conifer wood from the moderate conditions of Poland; (c) fresh conifer wood from the severe conditions of northern Sweden.

several million years. For such distant times, sea sediments, ice cores and corals lose much of their usefulness whereas petrified wood does not. Of course, we should keep in mind that the methodology of research should be modified in comparison with recent dendrological research. In the latter field, the search of long sequences of rings, matching the overlapping sequences and scaling by comparison with climatological databases are all possible. Meanwhile, new techniques will be demanded for the application of tree ring knowledge for petrified wood. The short- and long-scale internal standardization of the ring width and amplitude will probably play a key role in this new research.

The additional merit of our approach lies in establishing for the first time that at least three major branches of microspectroscopy, viz., electron microprobe, X-ray capillary microprobe and optical microprobe, may contribute to research in the field. Moreover, these methods complement each other, giving in many places analogous and in other places, more dependent on the surface conditions, different information. Especially, the auxiliary signals (bremsstrahlung in electron, scattered radiation in X-ray microprobes) give similar, density/wood structure-related information. Elemental information is clearly complementary—about the light elements from electron and about the heavy elements from X-ray microprobes. In our opinion, further investigation of the subject by the application of recent methods, supplemented with isotopic investigations and dating, should bring many other interesting results.

Acknowledgement

The authors are deeply grateful to Professor M. Matejak and Eng. M. Jablonski of the Main School of Farming, Agriculture Academy, Warsaw, and to Eng. Z. Kostrzewski of Zamosc, Poland, for supplying samples of petrified wood. We also thank Mr. H. Werner, a private collector at Hoevenen, Belgium, for the generous donation of samples from his collection. A. Kuczumow acknowledges a research grant from the Belgium Office for Scientific, Technical and Cultural Affairs.

References

- 1 *Methods of Dendrochronology*, ed. E. R. Cook and L. A. Kairiukstis, Kluwer, Dordrecht, 1990.
- 2 F. H. Schweingruber, *Tree Rings Basics and Applications of Dendrochronology*, Kluwer, Dordrecht, 1988.
- 3 P. I. Kuniholm, B. Kromer, S. W. Manning, M. Newton, C. E. Latini and M. J. Bruce, *Nature (London)*, 1996, **381**, 780.
- 4 C. Renfrew, *Nature (London)*, 1996, **381**, 733.
- 5 H. J. Bruins and J. van der Plicht, *Nature (London)*, 1996, **382**, 213.
- 6 J. E. Francis, *Palaentology*, 1986, **29**, 665.
- 7 H. C. Fritts, *Tree Rings and Climate*, Academic Press, London, 1976.
- 8 H. C. Fritts, *Reconstructing Large-Scale Climatic Patterns from Tree-Ring Data*, University of Arizona Press, Tucson, AZ, 1991.
- 9 K. R. Briffa, P. D. Jones, F. H. Schweingruber and T. J. Osborn, *Nature (London)*, 1998, **393**, 450.
- 10 J. W. Back, J. Recy, F. Taylor, R. L. Edwards and G. Cabiocch, *Nature (London)*, 1997, **385**, 705.
- 11 J. J. Labrecque and P. A. Rosales, *Spectrochim. Acta, Part B*, 1997, **52**, 1645.
- 12 W. Beck, *Science*, 1998, **279**, 1003.
- 13 M. K. Gagan, L. K. Ayliffe, D. Hopley, J. A. Cali, G. E. Mortimer, J. Chappell, M. T. McCulloch and M. J. Head, *Science*, 1998, **279**, 1014.
- 14 I. R. Quitmyer, D. S. Jones and W. S. Arnold, *J. Archeol. Sci.*, 1997, **24**, 825.
- 15 S. R. Hart and J. Blusztajn, *Science*, 1998, **280**, 883.
- 16 G. M. Thompson, D. N. Lumsden, R. L. Walker and J. A. Carter, *Geochim. Cosmochim. Acta*, 1975, **39**, 1211.
- 17 P. Holden, University of California, Santa Cruz, personal communication, 1998.
- 18 I. J. Winograd, T. B. Coplen, J. M. Landwehr, A. C. Riggs, K. R. Ludwig, B. J. Szabo, P. T. Kolesar and K. M. Revesz, *Science*, 1992, **258**, 255.
- 19 K. R. Ludwig, K. R. Simmons, B. J. Szabo, I. J. Winograd, J. M. Landwehr, A. C. Riggs and R. J. Hoffman, *Science*, 1992, **258**, 284.
- 20 R. L. Edwards, H. Cheng, M. T. Murrell and S. J. Goldstein, *Science*, 1997, **276**, 782.
- 21 J. M. Vadillo, I. Vadillo, F. Carasco and J. J. Laserna, *Fresenius' J. Anal. Chem.*, 1998, **361**, 119.
- 22 R. B. Alley, D. A. Meese, C. A. Shuman, A. J. Gow, K. C. Taylor, P. M. Grootes, J. W. C. White, M. Ram, E. D. Waddington, P. A. Mayewski and G. A. Zielinski, *Nature (London)*, 1993, **362**, 527.
- 23 W. Dansgaard, S. J. Johnsen, H. B. Clausen, D. Dahl-Jensen, N. S. Gundestrup, C. U. Hammer, C. S. Hvidberg, J. P. Steffensen, A. E. Sveinbjörnsdóttir, J. Jouzel and G. Bond, *Nature (London)*, 1993, **364**, 218.
- 24 G. A. Zielinski and M. S. Germani, *J. Archeol. Sci.*, 1998, **25**, 279.
- 25 D. W. Oppo, J. F. McManus and J. L. Cullen, *Science*, 1998, **279**, 1335.
- 26 H. Schulz, U. von Rad and H. Erlenkeuser, *Nature (London)*, 1998, **393**, 54.
- 27 A. Kuczumow, A. Rindby and S. Larsson, *X-Ray Spectrom.*, 1995, **24**, 19.
- 28 K. Pernestål, B. Jonsson and J. E. Hällgren, *Nucl. Instrum. Methods, Sect. B*, 1993, **75**, 326.
- 29 S. A. E. Johansson, *Analyst*, 1992, **117**, 259.
- 30 G. Loevestam, E. M. Johansson, S. Johansson and J. Pallon, *Ambio*, 1990, **19**, 87.
- 31 A. Kuczumow, S. Larsson and A. Rindby, *X-Ray Spectrom.*, 1996, **25**, 147.
- 32 A. M. Keller and M. S. Hendrix, *Palaeos*, 1997, **12**, 282.
- 33 G. T. Creber and W. G. Chaloner, *Palaeoecol. Palaeoclimatol. Palaeoecol.*, 1985, **52**, 35.
- 34 S. Carroll, E. Mroczek, M. Alai and M. Ebert, *Geochim. Cosmochim. Acta*, 1998, **62**, 1379.
- 35 H. Kumagai and Y. Fukao, *Geophys. Res. Lett.*, 1992, **19**, 1859.
- 36 H. Hicks, *US Pat.*, 4 612 050, 1986.
- 37 G. Scurfield and E. R. Segnit, *Sediment. Geol.*, 1984, **39**, 149.
- 38 R. W. Drum, *Science*, 1968, **161**, 175.
- 39 J. H. Oehler, *Geol. Soc. Am. Bull.*, 1976, **87**, 1143.
- 40 A. C. Sigleo, *Geochim. Cosmochim. Acta*, 1978, **42**, 1397.
- 41 C. Stein, *J. Sediment. Petrol.*, 1982, **52**, 1277.
- 42 K. Janssens, L. Vincze, J. Rubio and F. Adams, *J. Anal. At. Spectrom.*, 1994, **9**, 151.
- 43 K. Janssens, B. Vekemans, L. Vincze, F. Adams and A. Rindby, *Spectrochim. Acta, Part B*, 1996, **51**, 1661.
- 44 P. Chevallier, P. Dhez, F. Legrand, A. Erko, Y. Agafonov, L. A. Panchenko and A. Yakshin, *J. Trace Microprobe Technol.*, 1996, **14**, 517.
- 45 P. Dillman, P. Populus, P. Chevallier, P. Fluzin, G. Beranger and A. Firsov, *J. Trace Microprobe Technol.*, 1997, **15**, 251.
- 46 G. Andermann and J. W. Kemp, *Anal. Chem.*, 1958, **30**, 1306.
- 47 H. A. van Sprang and M. H. J. Bekkers, *X-Ray Spectrom.*, 1998, **27**, 31.
- 48 P. M. Van Dyck and R. E. Van Grieken, *Anal. Chem.*, 1980, **52**, 1859.
- 49 M. F. Aratijo, P. Van Espen and R. Van Grieken, *X-Ray Spectrom.*, 1990, **19**, 29.
- 50 S. A. E. Johansson, *Endeavour*, 1989, **13**, 48.
- 51 A. Kuczumow, B. Vekemans, M. Claes, O. Schalm, L. Vincze, W. Dorriné, K. Gysels and R. Van Grieken, *X-Ray Spectrom.*, accepted for publication.
- 52 G. Bond and R. Lotti, *Science*, 1995, **267**, 1005.
- 53 M. E. Raymo, K. Ganley, S. Carter, D. W. Oppo and J. McManus, *Nature (London)*, 1998, **392**, 699.
- 54 D. W. Stahle, M. K. Cleaveland, D. B. Blanton, M. D. Therrell and D. A. Gay, *Science*, 1998, **280**, 564.
- 55 S. L. de Silva and G. A. Zielinski, *Nature (London)*, 1998, **393**, 455.